Stomatal closure in maize is mediated by subsidiary cells and the PAN2 receptor

Le Liu, M. Arif Ashraf, Taylor Morrow, Michelle Facette*
Department of Biology, University of Massachusetts Amherst, Amherst, MA, USA
*Corresponding author, email: mfacette@umass.edu

ORCID:
LL: orcid.org/0000-0002-4262-5063
MAA: orcid.org/0000-0002-0879-5835
TM：orcid.org/0009-0003-5473-742X
MRF: orcid.org/0000-0002-6214-9359

Keywords: maize/stomata/subsidiary cells/guard cell

Abstract

Stomata are epidermal pores that facilitate plant gas exchange. Grasses have fast stomatal movements, likely due to their dumbbell-shaped guard cells and lateral subsidiary cells. Subsidiary cells reciprocally exchange water and ions with guard cells. However, the relative contribution of subsidiary cells to stomatal closure is unresolved. We compared stomatal gas exchange and stomatal aperture dynamics in wild type and *pan1*, *pan2*, and *pan1;pan2* maize (*Zea mays*) mutants, which have varying percentages of aberrantly formed subsidiary cells. Stomata with 1 or 2 defective subsidiary cells cannot close properly, indicating that subsidiary cells are essential for stomatal function. Even though the percentage of aberrant stomata is similar in *pan1* and *pan2, pan2* showed a more severe defect in stomatal closure. In *pan1*, only stomata with abnormal subsidiary cells fail to close normally. In *pan2*, all stomata have stomatal closure defects, indicating that PAN2 has an additional role in stomatal closure. Maize *Pan2* is orthologous to Arabidopsis thaliana *GHR1,* which is also required for stomatal closure. PAN2 acts downstream of Ca^{2+} in maize to promote stomatal closure. This is in contrast to GHR1, which acts upstream of Ca^{2+}, and indicates differently wired pathways in maize and Arabidopsis.

Introduction

Stomata are small pores on the leaf surface of land plants that facilitate gas exchange between the plant and the atmosphere. Acquisition of stomata and leaf cuticles was critical for plants to colonize the fluctuating terrestrial environment (Hetherington & Woodward, 2003). Open stomatal pores allow the absorption of carbon dioxide into the plant for photosynthesis, while simultaneously allowing oxygen and water vapor to diffuse out, facilitating plant transpiration. Stomata are responsible for ~80-95% of plant transpiration, depending on species and leaf water potential (Hanson *et al.*, 2016). Plants regulate stomatal opening and closing (i.e., regulate stomatal aperture) in response to exogenous and endogenous signals to balance water loss and carbon gain. Exogenous signals such as light, vapor pressure deficit (VPD), and CO_2 concentration regulate stomatal aperture (Eyland *et al.*, 2021). Endogenous signals that regulate stomatal aperture include phytohormones like abscisic acid (ABA), hydrogen peroxide (H_2O_2), nitric oxide (NO), and other mesophyll-derived metabolites (Suhita *et al.*, 2004). The time it takes for stomata to open or close in response to light cues is much greater than how long it takes for photosynthetic light reactions to be activated or stopped (Lawson & Blatt, 2014; Pearcy,1990). Therefore, photosynthetic capacity is often dictated by the rate of stomatal movement when light intensity is not limited. The kinetics of stomatal conductance (g_s) influences plant growth and water use efficiency in the field (Lawson and Blatt, 2014). It has been hypothesized that plants with faster stomatal kinetics have advantages in water use and photosynthesis efficiency in variable environments since steady-state values of g_s and assimilation under fluctuating conditions can be achieved rapidly (Lawson & Blatt, 2014; Vialet-Chabrand *et al.*, 2017; Eyland *et al.*, 2021; Long *et al.*, 2022).

Graminoid (grass) stomata have rapid stomatal responses relative to other plants (Raschke & Fellows, 1971; Grantz & Assmann, 1991; Franks & Farquhar, 2007; Vico *et al.*, 2011). The unique dumbbell-shaped guard cells and laterally associated subsidiary cells likely contribute to the fast graminoid stomatal movements (Franks & Farquhar, 2007; Gray *et al.*, 2020; Nunes et al., 2020; Hetherington & Woodward, 2003). The reciprocal exchange of potassium and chloride between subsidiary cells and guard cells

was first shown in maize (*Zea mays*) by Raschke and Fellows (Raschke & Fellows, 1971). This “see-saw” model of reciprocal flux of water and ions was further corroborated by Franks and Farquhar (Franks & Farquhar, 2007) and has been shown in barley (Schäfer *et al.*, 2018). Genetic evidence supporting the importance of subsidiary cells was first demonstrated via the *Brachypodium distachyon* mutant *sid1*, and shortly thereafter by the maize mutant *bzu2* (Raissig *et al.*, 2017; Wang *et al.*, 2019b)*. BdMUTE* and *ZmBzu2* are orthologous to the *Arabidopsis thaliana* transcription factor *AtMUTE.* In *A. thaliana*, MUTE is important for specification of guard cell fate (Pillitteri *et al.*, 2007). In *B. distachyon* and *Zea mays*, loss of MUTE results in a complete loss of subsidiary cells. Both grass mutants have defects in stomatal closure. However, *Bdsid1* and *Zmbzu2* also have defective guard cells to various extents, confounding the results (Raissig *et al.*, 2017; Wang *et al.*, 2019a). To directly assess the role of subsidiary cells, analysis of mutants in which guard cells are unaffected is warranted.

The mechanism of turgor-driven movement of guard cells has been well-researched using *A. thaliana* as a model (Jezek & Blatt, 2017; Lawson & Matthews, 2020; Hsu *et al.*, 2021). In *A. thaliana*, signals that trigger stomatal closure are typically mediated by ABA and core guard cell-specific kinases (Nunes *et al.*, 2020; Hsu *et al.*, 2021). Stomatal closure results from the activation of ion channels and transporters, including the slow-type anion channel (SLAC1), which allows the efflux of K+ and then lead to the water efflux and causing turgor decrease in the guard cells, which in turn leads to closure of the stomatal pore (Vahisalu *et al.*, 2008; Geiger *et al.*, 2009; Munemasa *et al.*, 2015). In Arabidopsis, SLAC1 is activated by the leucine-rich repeat receptor-like kinase (LRR-RLK) GUARD CELL HYDROGEN PEROXIDE-RESISTANT1 (GHR1), in addition to other signaling components such as the OST1 kinase (Hua *et al.*, 2012). The increase of cytosolic H_2O_2 and Ca^{2+} of guard cells acts as a molecular switch that modulates the activity of various ion channels, transporters, and enzymes involved in stomatal movement, leading to the closure of stomata and reducing water loss in plants (Hua *et al.*, 2012; Sierla *et al.*, 2018; Hsu *et al.*, 2021).

Stomatal closure is stimulated by, ABA, H_2O_2 and Ca^{2+} in maize just as is in *A. thaliana*. Notably, more cytosolic H_2O_2 and Ca^{2+} accumulates in subsidiary cells than in guard cells during maize stomatal closure (Yao *et al.*, 2013; Zhang *et al.*, 2020). This raises the question of how subsidiary cell turgor is regulated. Subsidiary cells have opposite turgor and ion fluxes to guard cells, but how does this occur? Are there different channels and/or regulatory proteins in subsidiary cells, or are the same mechanisms in guard cells employed in subsidiary cells? Are guard cells primarily regulated, and subsidiary cells merely responsive to the changes in the adjacent guard cells, perhaps accumulating potassium and calcium the guard cells export into the apoplast? Previous analyses have identified proteins shared between grass subsidiary and guard cells, as well as those that are unique to each cell type (Majore *et al.*, 2002; Mumm *et al.*, 2011; Nguyen *et al.*, 2017; Sun *et al.*, 2022). None-the-less, whether the two cell types have unique signaling mechanisms, and what if any coordination exists between subsidiary cells and guard cells is still unclear.

To understand the relative roles of subsidiary cells to the stomatal closure, we assayed stomatal function using previously characterized maize mutants which have defects in subsidiary cell formation. The *pan1* and *pan2* mutants have subsidiary cell specific defects in division plane orientation, leading to abnormally shaped subsidiary cells that are often not correctly specified (Gallagher & Smith, 1999; Zhang *et al.*, 2012). Both genes encode catalytically inactive leucine rich repeat receptor like kinases (LRR-RLKs). Despite their similar names, *pan1* and *pan2* are not paralogs. They share a gene name because they were discovered in the same screen. We found that stomatal complexes with abnormal subsidiary cells impaired stomatal closure, indicating an essential role for subsidiary cells. Moreover, PAN2, as its one-to-one orthologue GHR1, plays essential roles in the grass stomatal closure. Overall, our study provides insights into the relative roles of subsidiary cells and guard cells in stomatal closure and highlights the importance of PAN2 in the grass stomatal closure.

Materials and Methods

Plant materials and Growth Conditions

Maize mutants *pan1-ems* (Cartwright *et al.*, 2009), *pan2-O* and *pan2-2* (Zhang *et al.*, 2012) and *pan1-Mu;pan2-O* (Zhang *et al.*, 2012) have been previously described. All mutants were backcrossed at least five times into the B73 wild-type background. B73 inbred lines were used as controls in all experiments. PAN1-YFP and PAN2-YFP transgenic plants were described previously (Humphries *et al.*, 2011; Zhang *et al.*, 2012). These are genomic constructs with the native promoter and terminator. All the plants used in this study were grown in a greenhouse between 20°C and 29°C with supplemental LED light (Fluence VYPR series) (16-hour day length). Plants were grown in Pro-mix Professional soil supplemented with Peters Excel 15-5-15 CalMag fertilizer and chelated liquid iron (Southern Ag) as needed.

Gas exchange measurements

Stomatal conductance measurements were performed using a CIRAS3 gas analyzer equipped with a PCL3 leaf cuvette (PP Systems). For all measurements, healthy, fully expanded leaves were used. Briefly, the leaf cuvette was clamped onto the leaves and equilibrated for at least 30 mins to stabilize the initial stomatal conductance at 1000 PPFD. The CO_2 concentration was held constant at 410 parts per million (ppm); H_20 reference was set to 80%; and the cuvette flow at 300 cc min^{-1} . Stomatal conductance (g_s) and assimilation (A) rates were measured every 5 seconds during the entire treatment period. To measure stomatal closure rates, lights were turned off (PPFD=0) after the initial conductance became stable. For CO_2 responses, after the initial stomatal conductance was steady, and CO_2 concentration was shifted from 410 ppm to 2,000 ppm. Relative g_s was computed for each individual measured plant by normalizing g_s to the initial steady state g_s value observed. Data analysis was performed in R and JMP® 16.1. The data presented are the mean ± standard error of at least five leaves per treatment.

Stomatal phenotyping

Epidermal glue impressions were performed on full expanded leaf 3, 5 or 8 according to (Allsman et al., 2019). Morphology of guard and subsidiary cells was examined via

confocal microscopy (described below). Plants were fixed in formaldehyde-alcohol-acetic acid (FAA) and then stained with 0.1% Direct Red and 0.1% Calcofluor

Stomatal aperture assays

All the leaves we included in the stomatal aperture experiment were healthy and fully expanded. Maize leaf blade segments from leaf 5 or leaf 8 were floated in opening buffer (10 mm KCl, 50 µm $CaCl_2$, and 10 mm MES/Tris, pH 5.6) in the absence or presence of 10 mM ABA under light (500-700 PPFD). For Ca^{2+} treatment experiments, the epidermis was peeled from fully expanded L4 and immediately floated in the opening buffer in the absence or presence of 100 µm $CaCl_2$ under light. Leaves were treated for 2 hours; then, the leaves were stained using 1mM Propidium iodide (PI) for 15 mins (whole leaf piece) or 1 min for peels. The stomatal apertures were immediately observed under a confocal microscope (described below) and measured using FIJI software (Schindelin *et al.*, 2012).

Gene Expression Analysis by qRT-PCR

RNA was extracted from the division zone and different leaf samples from greenhouse-grown corn plants using RNeasy® Plant Mini Kit (Qiagen). Extracted RNA concentrations were quantified using a NanoDrop (Thermo Scientific). Each RNA concentration was normalized with RNase-free water, and 500 ng RNA was used to synthesize cDNA using ProtoScript® II Reverse Transcriptase (NEB). Quantitative PCR reactions were performed using StepOnePlus™ Real-Time PCR System (Applied Biosystems) and PowerUpTM SYBR™ Green Master Mix (Applied Biosystems). The reaction was performed as per the manufacturer's instructions. For quantification of gene expression, we used the $2^{-\Delta\Delta CT}$ (cycle threshold) method with normalization to the UBCP expression. Data were obtained from three biological replicates (independent plants) and two technical replicates. Primers used in this study are listed in Supplemental Table 1.

Plasmolysis

Leaf blade segments from fully-expanded maize leaf 4 expressing PAN2-YFP were submerged into 500 mM mannitol for 10 mins. Segments were then mounted in 500 mM mannitol and immediately observed using confocal microscopy.

Confocal Microscopy

Plant tissues were observed using a custom-built spinning disc confocal unit (3i) equipped with an inverted fluorescence microscope (IX83- ZDC, Olympus) CSU-W1 spinning disc with 50-micron pinholes (Yokogawa), a Mesa Illumination Enhancement 7 Field Flattening unit (3i), an Andor iXon Life 888 EMCCD camera, a UPLANSAPO60XS2 (NA = 1.20, Olympus) or UPLANSAPO40X (NA = 1.25, Olympus) Silicone Oil Immersion objective and 4 laser stack with TTL controller (3i). For YFP imaging of transgenic maize plants, the 514 nm laser and 542/27 emission filter (YFP) were used. The 568 laser with 618/50 emission filters were used for PI and Direct Red staining experiments. Image processing was performed using Image FIJI and Adobe Photoshop version 8.0. The YFP fluorescence intensity was qualitatively measured using FIJI. Max projections of six slices of 16-bit images taken on the same day with the same acquisition settings were used. Sibling plants without YFP fluorescence were used as controls.

Accession Numbers

Gene and protein sequences for maize and Arabidopsis can be found at MaizeGDB (www.maizegdb.org) and TAIR (https://www.arabidopsis.org/index.jsp), respectively. Accession numbers for maize Version 5.0 of the V73 genome are: PAN1 (Zm00001eb034900), and PAN2 (Zm00001eb117610).

Statistical Analyses

Non-parametric comparisons for each pair using Wilcoxon Methods were performed to compare the stomatal aperture. Summary statistics for stomatal aperture are listed in Supplemental Table S2 and results of statistical tests are in Supplemental Table S3. Student's t-test was used to compare the percentage of abnormal stomata and qPCR value. Raw CT value used for statistical test is in Supplemental Table 4, and the results of the T-tests are listed in Supplemental Table 5. All statistical tests were performed in JMP® 16.1.

Results

The percentage of abnormal stomatal complexes varies across different genotypes and leaves

What is the relative contribution of subsidiary cells in grass stomatal function? Are subsidiary cells a passive reservoir that accumulate ions and water because of their proximal location to guard cells, or do they actively promote stomatal function? PANGLOSS1 (PAN1) and PAN2 were previously identified as LRR-RLKs in maize that are polarized prior to the formative divisions that generate subsidiary cells during stomatal development (Cartwright *et al.*, 2009; Zhang *et al.*, 2012). Both *pan1-ems* and *pan2-2 are* null mutants that have incomplete penetrance, where only a portion of subsidiary cells are abnormal in the single mutants (Cartwright et al., 2009; Zhang et al., 2012; Figure 1). The percentage of abnormal subsidiary cells varies by leaf number in *pan1* and *pan2* (Figure 1). Leaves that emerge first have a higher frequency of subsidiary cell defects, while later-emerging leaves have fewer defective cells. Previous analyses suggest that morphologically correct subsidiary cells are likely correctly specified (Gallagher & Smith, 1999). We are unable to propagate the more severe *pan1-ems;pan2-2* double mutants, so the weaker alleles of *pan1-mu* and *pan2-O* were used to generate *pan1-mu;pan2-O.* The *pan1;pan2* double mutant has a synergistic phenotype, with more than double the frequency of abnormal subsidiary cells than either of the single mutants (Zhang *et al.*, 2012; Figure 1).

To visualize guard cell and subsidiary cell morphology, we generated three-dimensional images of the stomata in four genotypes using confocal microscopy. In *pan1-ems*, *pan2-2*, and *pan1;pan2*, all guard cells are correctly formed and have a characteristic dumbbell-shape (Figure 1). Therefore, these mutants provide a genetic tool to specifically assay subsidiary cell contributions to stomatal function, without the confounding effects of improper guard cell specification. The cell divisions that specify the two subsidiary cells in a stomatal complex are independent of each other, therefore any given stomatal complex may have 0 abnormal (i.e., normal), 1 abnormal, or 2 abnormal subsidiary cells. We classified the frequency of abnormal complexes in the 4 genotypes in leaf 3, leaf 5 and leaf 8. (Figure 1). The percentage of stomatal

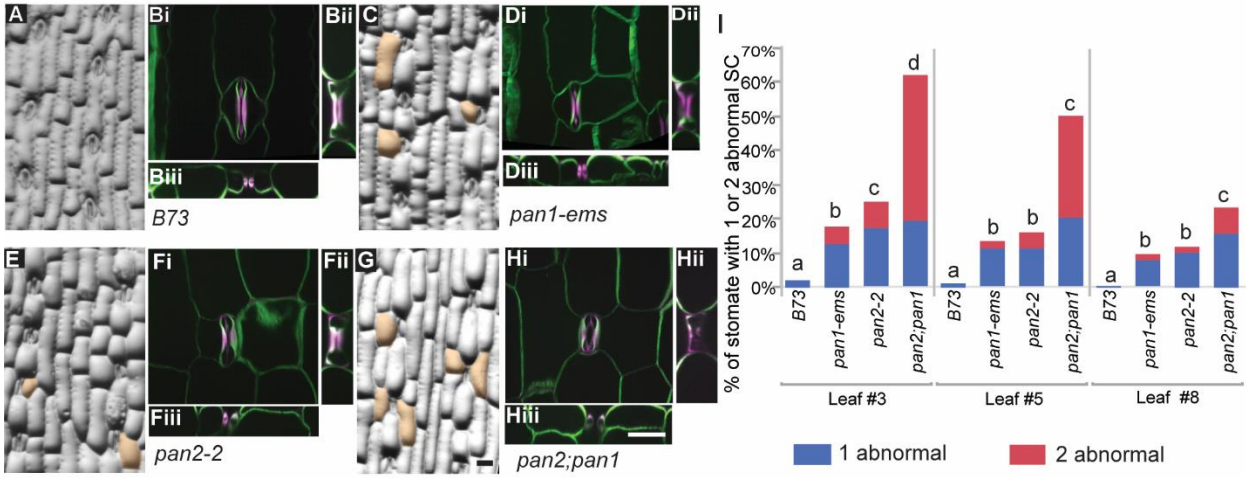

Figure 1: Mature subsidiary cells are abnormal in *pan1*, *pan2,* and *pan2;pan1* mutants. Epidermal glue impressions (A, C, E, G) and confocal images (B, D, F, H) of wild type (A, B), *pan1* (C,D), *pan2* (E,F), and *pan2;pan1* (G,H). Abnormal subsidiaries are false-colored orange in the glue impressions. The confocal images show individual stoma stained with direct red (magenta) and calcofluor (green) and include reconstructed orthogonal views in the x (right of image) and y (below image) planes, which show the characteristic dumbbell shape of the guard cells. (E) Percentage of stomatal complexes with abnormal subsidiary cells in leaf 3, 5, and 8. Genotypes with different letters represent the percentage of stomata with one and two abnormal subsidiary cells that are significantly different from each other ($p \leq 0.05$). Statistical analysis is performed based on the student's t-test. All the representative pictures are from leaf 5. Images A, A, C, E & G are at the same scale. Images B, D, F, & H are at the same scale. Scale bars in G and H are both 50 µm.

complexes with improper subsidiary cell divisions (and therefore misspecified subsidiary cells) decreased as the leaf number increased. In leaf 3 of *pan1-ems* and *pan2-2*, ~25% of stomata have abnormal subsidiary cells, but this decreases to ~20 % in leaf 5 and ~10% in leaf 8. In leaf 3 of the *pan1;pan2* double mutant, more than 60% of the stomatal complexes have one or two abnormal subsidiary cells, and the percentage of abnormal cells decreases in leaf 5 and 8. This broad range of defective subsidiary cell percentages across different genotypes and leaf numbers, coupled with normal guard cells, provides a useful tool to specifically assay subsidiary cell function during stomatal closure.

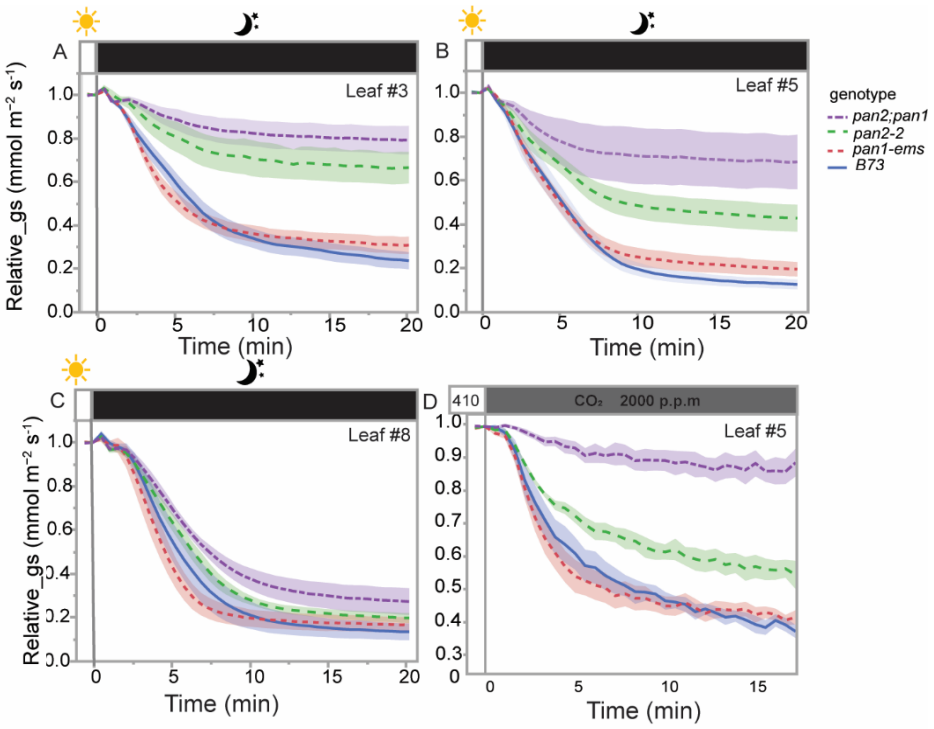

Figure 2. Stomatal closure is impaired in *pan2;pan1*, and *pan2* but is normal in *pan1*. Normalized stomatal conductance (g_s) of *pan2*, *pan2;pan*1, *pan1*, and B73 in response to darkness in leaf 3 (A), leaf 5, (B), or leaf 8 (C) was measured over time. PPFD was changed from 1000 to 0 at time zero. (D) Normalized stomatal conductance (g_s) in leaf 5 in response to elevated CO_2 was measured over time. The CO_2 concentration of from 410 ppm to 2000 ppm at zero time. Measurements were taken every 5 seconds. Relative g_s was computed for each measured plant by normalizing g_s to the observed steady initial g_s value. The data presented are the mean ± SE of at least 5 individual plants.

Loss of PAN2, but not PAN1, impairs stomatal closure as inferred by gas exchange

We hypothesized that if subsidiary cells play a critical role in maize stomatal function, the *pan1* and *pan2* single mutants would have moderate defects in stomatal closure. We predicted that the *pan1;pan2* double mutant would exhibit more severe defects in stomatal closure, since *pan1;pan2* has more defective stomatal complexes. Furthermore, we predicted that the earliest emerging leaves, which have the highest frequency of abnormal subsidiary cells, would have the strongest stomatal closure defect; and that later emerging leaves would have subtle or no stomatal closure defects.

We assayed stomatal closure by measuring g_s via gas exchange measurements in wild type and mutant plants in response to the darkness (Figure 2A-C). We measured

g_s in leaf 3, leaf 5 and leaf 8 in B73 (wild type control), *pan1*, *pan2*, and *pan1;pan2.* In B73 control plants, g_s shows a characteristic inverted sigmoidal curve that indicates stomatal closure in response to darkness. As predicted, *pan1;pan2* double mutants showed a stomatal closure defect in response to darkness across all leaves (Figure 2). Moreover, *pan1;pan2* showed milder defects as the leaf number increased, also consistent with our hypothesis. Surprisingly, *pan1* and *pan2* showed different responses from each other, even though they have the same percentage of abnormal subsidiary cells. Consistent with our prediction, *pan2* showed a defect in stomatal closure that is milder than *pan1;pan2*. On the other hand, *pan1* had no defect in stomatal closure. Importantly, even though *pan1* has no observable defect in dark-induced stomatal closure on its own, the *pan1;pan2* double mutant has a more severe impairment than *pan2-2.* This indicates that even though *pan1* did not have a detectable stomatal closure phenotype as measured by g_s, subsidiary cell specification as influenced by *pan1* is still important for stomatal closure.

To determine if the stomatal closure defect in *pan2* and *pan1;pan2* was specific to darkness-induced closure or a more general defect, we tested another environmental cue that promotes stomatal closure. If the defect is caused by defective subsidiary cells, we reasoned the defect should persist independent of the cue. We increased CO_2 concentration from 410 ppm (parts per million) to 2,000 ppm to induce stomatal closure. Similar to stomatal closure induced by darkness, *pan2* and *pan1;pan2* showed moderate and strong defects in stomatal closure, respectively, in response to elevated CO_2 (Figure 2). We did not observe a defect in stomatal closure in *pan1* in response to darkness or elevated CO_2 (Figure 2).

We confirmed the defect in stomatal closure in *pan2* by analyzing a second, weaker allele of *pan2* (Supplemental Figure S1). The *pan2-O* mutant contains a missense mutation that results in a Ser to Phe change near the N terminus of the protein, which results in less PAN2 protein (Zhang et al., 2012). The percentage of abnormal subsidiary cells in *pan2-O* is less than in *pan2-2* (Supplemental Figure S1A). Both alleles showed impaired stomatal closure relative to B73, and *pan2-O* shows a

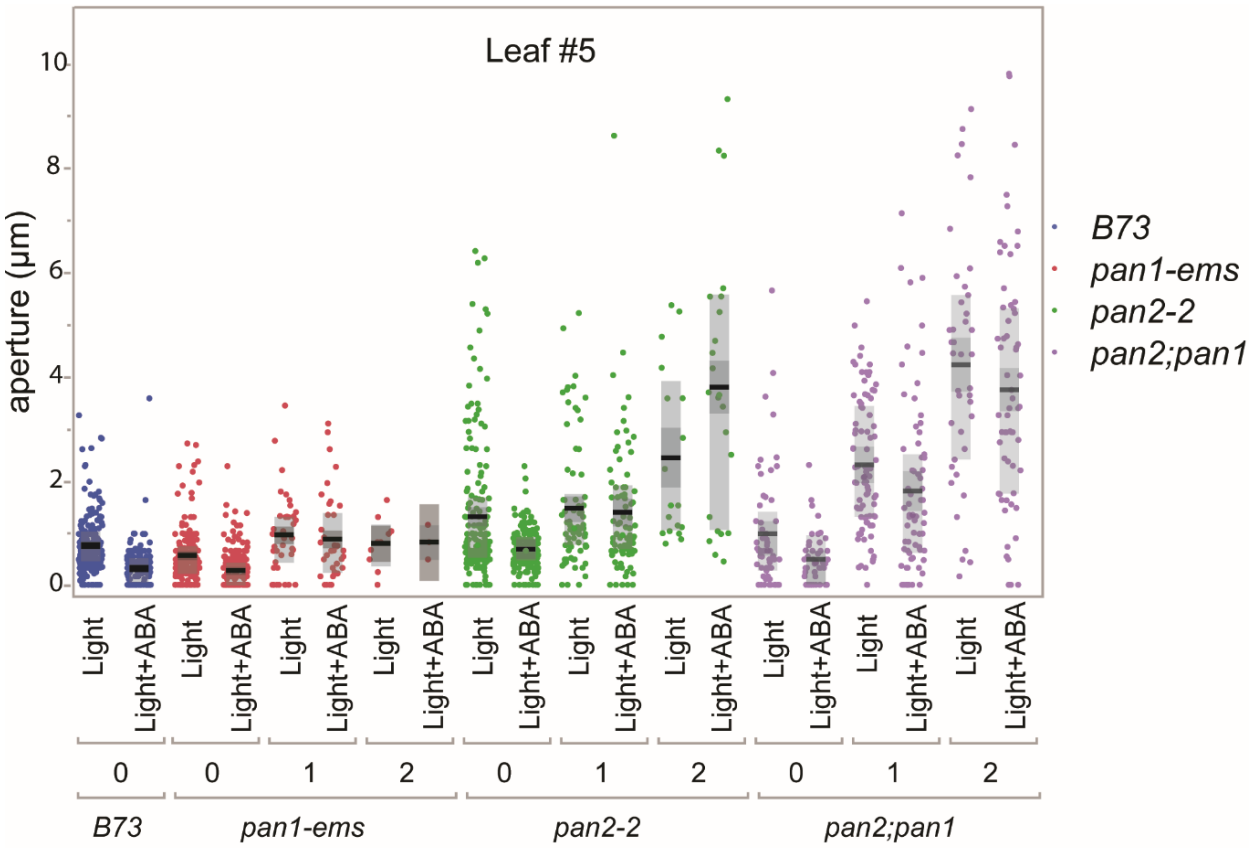

Figure 3. Stomatal aperture of different genotypes of leaf 5 in response to ABA. Fully expanded leaf 5 segments from B73, *pan1, pan2,* or *pan2;pan1* were incubated in opening buffer under 500 µm/m²/s light, without or with the addition of 10 mM ABA. After 2 hours, the pieces were stained with propidium iodide (PI) and imaged on the confocal microscope. Stomata were classified as having 0 abnormal (i.e., normal), 1 abnormal, or 2 abnormal subsidiary cells and stomatal apertures were measured. Each data point represents a single stomatal complex, with 4-5 plants per genotype & treatment were used.

milder defect than *pan2-2* (Supplemental Figure S1B). These results are consistent with *pan2-O* being a weaker allele (Zhang et al., 2012).

PAN2 contributes to stomatal function in two distinct ways

Our observation that *pan2*, but not *pan1*, has an effect on stomatal closure was perplexing, given they have a similar frequency of defective stomata. Stomatal gas exchange (g_s) is assayed on a population scale (many thousands of stomatal complexes). Notably, leaf 8 has almost normal stomatal closure, even in the double mutant. It is plausible that on a population level, impairment of stomatal closure of individual defective stomates are masked when the proportion of abnormal stomata is low. To determine if individual stomates with 0, 1, or 2 abnormal subsidiary cells are

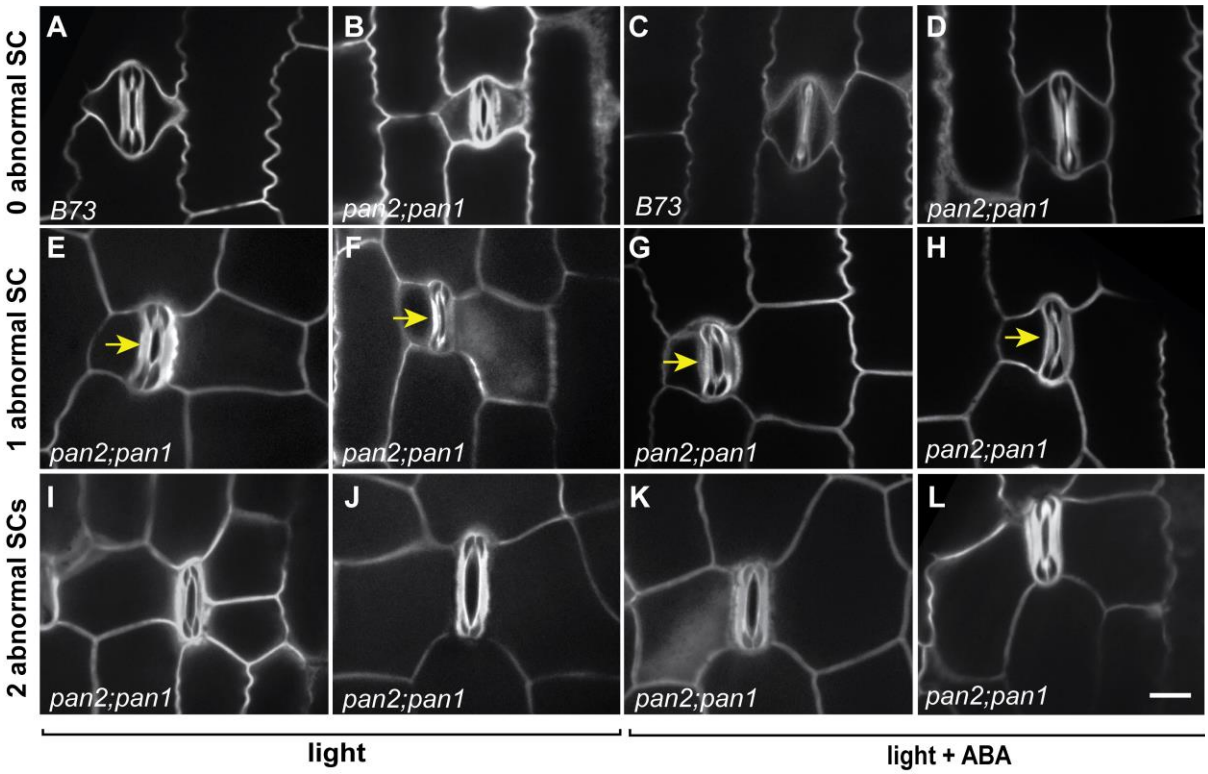

Figure 4. Curved guard cells imply that subsidiary cells exert a positive force
Leaf pieces of fully expanded leaves were treated in opening buffer in the presence or absence of 10 mM ABA. The stomata are classified into three categories based on the subsidiary morphologies. Stomata with 1 or 2 abnormalities failed to close in response to ABA treatments. The guard cells in the stoma complex with 1 abnormal subsidiary cell are curved, and all the curves are away from the normally formed subsidiary. The scale bar in L is 20 μm.

able to close normally, we treated leaf segments from mature leaf 5 with ABA, and assessed the impact of subsidiary cells on stomatal aperture by confocal microscopy (Figure 3). We measured stomatal aperture in leaf 5 (Figure 3) and leaf 8 (Supplemental Figure S2). Because of the substantial number of comparisons, we included summary data statistics in Supplemental Table S2 and results of pairwise non-parametric tests in Supplemental Table S3. Wild type stomata in B73 decreased in aperture upon treatment with ABA. Consistent with our observation, normally formed stomata in *pan1-ems* also responded to ABA. However, in *pan1* mutants with 1 or 2 abnormal subsidiary cells, the aperture prior to ABA treatment was slightly larger, and there was no appreciable decrease in stomatal aperture upon ABA treatment (Figure 3; Supplemental Tables S2 and S3). This indicates that even though *pan1* did not show a phenotype on a population level, individual stomates with defective subsidiary cells fail

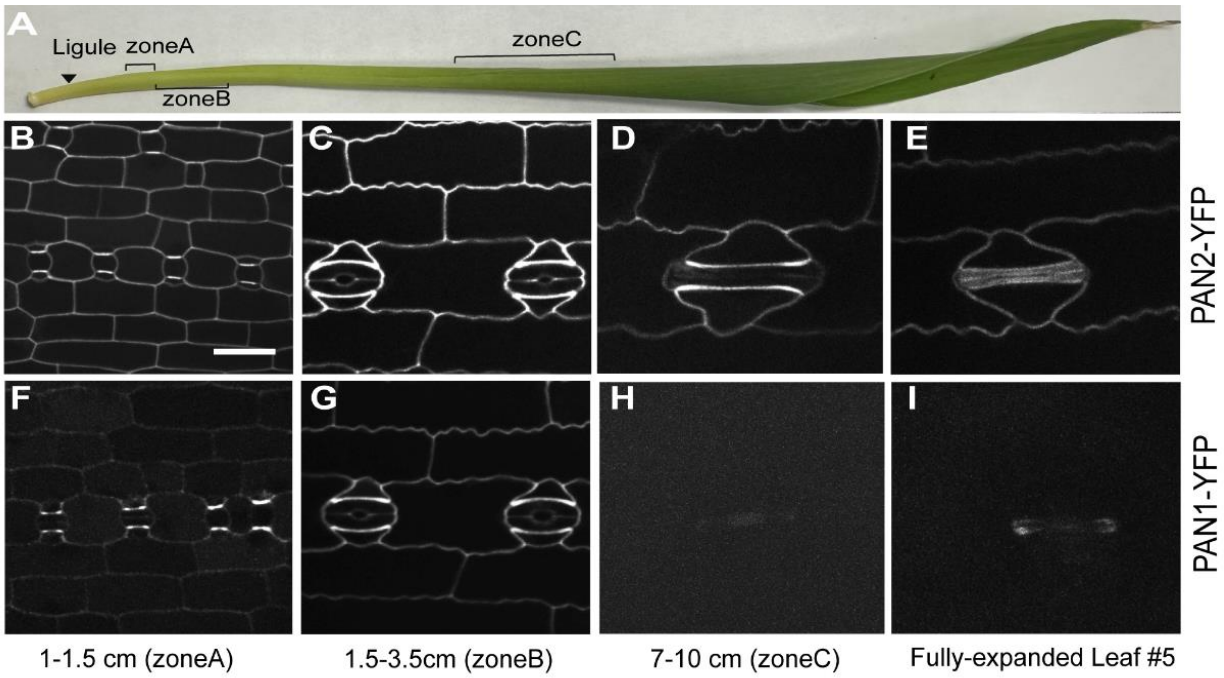

Figure 5 PAN1 and PAN2 have different expression patterns in stomatal division zones and fully expanded leaves. The outer leaves of 15-d-old plants expressing either PAN2-YFP (B-D) or PAN1-YFP (F-H) were removed to expose partially expanded leaf 5, where the developing ligule was within 0.5 dm of the leaf base. Leaf 5 was cut into 4 sections as illustrated in A to examine expression in partially expanded leaves. The leaf blade of a fully expanded leaf 5, where the leaf sheath and leaf blade are no longer growing, were examined for PAN2-YFP (E) or PAN1-YFP (I) expression. All images at the same scale; scale bar in A represents 20 µm.

to close properly, and supports the hypothesis that subsidiary cells directly participate in stomatal closure.

In *pan2* and *pan1;pan2* mutants, stomata with aberrant subsidiary cells fail to close properly, similar to *pan1.* Additionally, in *pan2* mutants, stomata with 0 abnormal subsidiary cells respond to ABA. However, *pan2* mutants, but show a significantly larger aperture in both the absence or presence of ABA relative to both *pan1* and *B73* (Figure 3). This indicates that PAN2 has an additional role in regulating stomatal aperture, independent of the roles PAN1 and PAN2 play during formative subsidiary cell divisions. Together, this indicates PAN2 regulates grass stomatal closure in two ways. Firstly, PAN1 and PAN2 both promote correct subsidiary cell formation during development, which is essential for stomatal closure. Secondly, PAN2 has an additional function in regulating stomatal aperture in all stomata, regardless of whether the subsidiary cell has divided correctly, via an unknown mechanism.

Subsidiary cells are essential for stomatal closure

Our stomatal aperture measurements in response to ABA allowed us to directly observe stomata with normal and abnormal subsidiary cells. We noticed that in stomata with one abnormal subsidiary cell and one normal cell, the guard cells tended to be curved away from the normal subsidiary cell (Figure 4). In *pan1;pan2*, we observed that 75% (76/101) of guard cells are curved in stomatal complexes with one abnormal subsidiary cell; and all of the curved subsidiary cells are away from the correct subsidiary cells (Figure 4). Similarly, 68% (13/19) of *pan1* and 73% (41/65) of *pan2* stomatal complexes with a single defective subsidiary cell curved away from the morphologically normal cell. This qualitative observation implies a pushing or positive force is generated from the normally formed subsidiary cell that results in stomatal pore closure, and suggests a direct mechanical role for subsidiary cell function.

PAN2, but not PAN1, is expressed in mature stomata

We further investigated the role of PAN2 in stomatal closure. The one-to-one orthologue of PAN2 in *A. thaliana* is *GUARD CELL HYDROGEN PEROXIDE RESISTANT 1 (GHR1)* (Hua *et al.*, 2012; Sierla *et al.*, 2018; Man *et al.*, 2020). In mature leaves, *GHR1* is expressed in guard cells but not in other mature epidermal cells (Hua *et al.*, 2012). GHR1 regulates stomatal closure in response to several environmental cues including hydrogen peroxide, light, and ABA (Hua *et al.*, 2012). GHR1 activates the S-type anion channel SLAC1 (Hua *et al.*, 2012; Sierla *et al.*, 2018). There is no evidence indicating that GHR1 plays a role in stomatal development. Our observation that PAN2 (but not PAN1) is required for stomatal closure, even in correctly divided subsidiary cells, suggests that PAN2 plays a functional role in mature stomata. Is PAN2 expressed in mature stomates like GHR1? If so, is PAN2 present in guard cells or subsidiary cells? We compared PAN1 and PAN2 expression patterns in developing and mature stomata. We examined leaves expressing PAN1-YFP and PAN2-YFP at multiple developmental stages using previously characterized marker lines (Humphries *et al.*, 2011; Zhang *et al.*, 2012; Sutimantanapi *et al.*, 2014). At the base of a partially expanded immature maize leaf, formative divisions that create stomata occur (Facette *et al.*, 2015). There is a developmental gradient from the base of the leaf to the tip, with

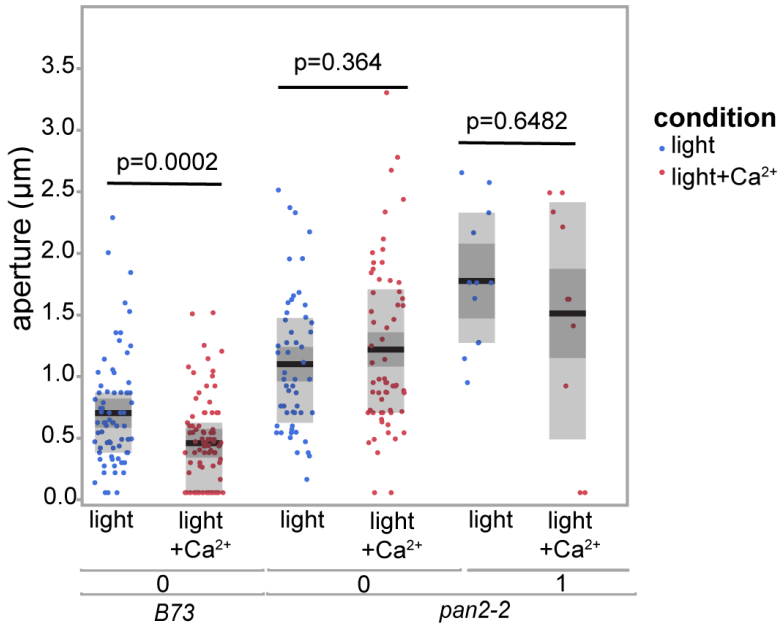

Figure 6.Stomatal aperture in *pan2* does not decrease in response to exogenous Ca^{2+}. Leaf tissue from *B73* or *pan2* was incubated in opening buffer or buffer supplemented with 100 µM Ca^{2+} under 500 µm/m²/s light. After 2 hours, the pieces were stained with propidium iodide (PI) and imaged on the confocal microscope. Stomatal apertures were measured from the images using FIJI. Stomata were classified as having 0 abnormal (i.e., normal), 1 abnormal subsidiary cells.

fully functional stomata at the leaf tip. We examined PAN1-YFP and PAN2-YFP expression along the leaf base at different points. Consistent with past findings, PAN1-YFP and PAN2-YFP polarize in pre-mitotic subsidiary mother cells at the site of guard mother cell contact, and remain polarized after division (Figure 5; Cartwright *et al.*, 2009; Zhang *et al.*, 2012; Sutimantanapi *et al.*, 2014). During cell differentiation and expansion, both PAN1-YFP and PAN2-YFP are expressed, again consistent with previous results (Sutimantanapi *et al.*, 2014). PAN1-YFP was undetectable in the leaf tip and mature leaves, with the only signal coming from autofluorescence (Figure 5). Note the heavily lignified guard cells autofluoresce strongly (Figure S3). At the tip of partially expanded leaf 5 and in fully expanded leaf 5, PAN2-YFP was clearly expressed in subsidiary cells and pavement cells (Figure 5). PAN2-YFP is no longer polarized in subsidiary cells, but is still present. Due to the guard cell autofluorescence, it was difficult to definitely conclude whether PAN2-YFP was present in guard cells. To address this we performed plasmolysis experiments. Again, PAN2-YFP was clearly expressed in subsidiary cells, and not seen in the central portion of the guard cells (the “handles” of the barbell) (Figure S3). We sometimes saw fluorescence in the bulbous

ends of the guard cells, but this was inconsistent and difficult to resolve from autofluorescence. Therefore, we concluded that like GHR1, PAN2 is expressed in the stomatal complex. PAN2 is expressed in subsidiary cells, and may also be expressed in guard cells. Our PAN1-YFP data indicates that PAN1 is not expressed in mature stomatal complexes (Figure 5) .

We further corroborated the expression of PAN2 and PAN1 in leaves via qPCR. Previous proteomic data indicated the presence of both proteins in immature leaves, but neither was detected in mature leaves (Facette *et al.*, 2015). This could be due to a low abundance of PAN2 in mature leaves, coupled with the relative insensitivity of proteomic detection. We performed quantitative real-time PCR (qRT-PCR) in different leaf numbers and division zones, using the mutants as a negative control. Both *PAN1* and *PAN2* are expressed in leaves where stomatal divisions and cell expansion are occurring (Supplemental Figure S5; Supplemental Tables S4 and S5). PAN2 is expressed in fully expanded leaf 3, 5 and 8, albeit at low levels. Nonetheless, the amount of expression was greater than what was detected in the null mutant. This is consistent with PAN2 having a role in stomatal function after development has completed. PAN1 expression in fully expanded leaves was similar to the null mutant (Supplemental Figure S5; Supplemental Tables S4 and S5). Together, these data indicate PAN2, but not PAN1, is expressed in mature stomata, consistent with a role for only PAN2 during stomatal function.

PAN2 regulates stomatal closure via a Ca^{2+}-dependent pathway.

In *A. thaliana*, *ghr1* is insensitive to dark-, CO_2-, and ABA-induced stomatal closure (Hua *et al.*, 2012), similar to *pan2*. Application of exogenous Ca^{2+} results in stomatal closure in wild type plants and restores stomatal closure in *ghr1,* which indicates that Ca^{2+} acts downstream of GHR1 in A. *thaliana* (Hua *et al.*, 2012; Sierla *et al.*, 2018). Given the phenotypically similar impairment of stomatal closure observed in *ghr1* and *pan2*, we wanted to test if the *pan2* phenotype could also be rescued by exogenous application of Ca^{2+}. We treated epidermal peels of B73 and *pan2-2* using the opening buffer previously described, in the presence or absence of 10 mM $CaCl^{2+}$ under 500-700 PPFD light. Consistent with our previous observation, *pan2-2* shows

larger stomatal apertures than B73 in both conditions (Figure 6). Application of exogenous Ca^{2+} induced stomatal closure in B73. Strikingly, *pan2* did not respond to application of exogenous Ca^{2+} (Figure 6). This suggests that the molecular pathway that PAN2 participates in may be differently wired in maize vs *A. thaliana,* and that in maize Ca^{2+} is upstream, rather than downstream, of PAN2.

Discussion

Properly formed subsidiary cells are essential for stomatal movements in maize

Stomata facilitate gas exchange for carbon dioxide absorption and drive plant transpiration, but are also the main source of plant water loss. The fast movements of grass stomata are attributed to the combination of subsidiary cells and dumbbell-shaped guard cells (Franks and Farquhar, 2007). Subsidiary cells are not unique to grasses (Gray et al., 2020). Substantive evidence across many plant species supports that subsidiary cells, or even neighboring pavement cells, accumulate ions in a manner opposite to guard cells during stomatal movement (Raschke & Fellows, 1971; Willmer & Pallas Jr., 1973; Dayanandan & Kaufman, 1975). However, subsidiary cells do not seem to be necessary for stomatal movements in all species. For example, in *Commelina communi*, which has lateral and polar subsidiary cells, stomata respond in the absence of living subsidiary cells (Squire & Mansfield, 1972). Franks and Farquhar (2007) convincingly showed that turgor changes in grass subsidiary cells oppose the turgor changes in guard cells, and there are subsidiary cell-specific ion channels (Majore *et al.*, 2002; Büchsenschütz *et al.*, 2005). Our gas exchange and microscopic analyses of genetically ablated subsidiary cells, at varying percentages, confirm that subsidiary cells are essential for stomatal closure in maize. In particular, the striking observation of curved guard cells in stomatal complexes with a single aberrant subsidiary cell indicates a positive force exerted by subsidiary cells that promotes closure. It is important to be aware that *pan2* has a subsidiary cell morphological defect not shared by *pan1* (Sutimantanapi *et al.*, 2014). Subsidiary cells in *pan2* have “flat sides”. However, we feel it is unlikely this flat-sided defect is unlikely to be the source of the *pan2* stomatal closure defect for two reasons. Firstly, flat-sided subsidiary cells

occur naturally in grasses lacking epidermal crenulations, such as *B. distachyon.* Secondly, and more importantly, our microscopic data indicates that in *pan2* and *pan1;pan2* stomatal complexes with a single abnormally divided subsidiary cell, the other subsidiary cell still exerts a positive or pushing force.

Individual abnormal stomates observed microscopically in *pan1* mutants have closure defects, however gas exchange data did not detect a defect. Because *pan1;pan2* double mutants showed a more severe defect than the *pan2* single mutant, *pan1*-induced subsidiary cell misspecification is a factor in stomatal closure. Later emerging leaves in *pan2* and *pan1;pan2,* which have fewer abnormal stomata than early leaves, also show mild to no defect. Hence it is plausible that a certain threshold percentage of abnormal stomata is required to show a population-level defect.

PAN2 is required for stomatal function in maize

Some studies have shown that subsidiary cells may participate in stomatal regulation signaling pathways. The subsidiary-cell-specific expressed glucose transporter CST1 is positively regulated in stomatal opening (Wang *et al.*, 2019b). The *cst1* mutant showed reduced stomatal opening, starvation, and early senescence, suggesting the necessary role for subsidiary cells in stomatal function or signaling mechanisms, although the mechanism behind this is unclear (Wang *et al.*, 2019b). It was also shown that the common signaling messenger H_2O_2 accumulated in the subsidiary cells and is necessary for drought-induced stomatal closure in maize, demonstrating the significance of stomatal signaling mechanisms (Yao *et al.*, 2013; Zhang *et al.*, 2020). Once again, the detailed mechanism of the subsidiary cell anatomy, membrane transporters, and their relationship with the guard cell behavior is still unclear. It is clear however that the SLAC1 transporter in grasses functions differently than in *A. thaliana*, as it has a requirement for nitrate (Schäfer *et al.*, 2018).

A strong connection between GHR1 and apoplastic ROS has been suggested (Hua et al., 2012; Devireddy et al., 2018), and genetic analysis indicated that GHR1 acts downstream of ROS production but upstream of Ca^{2+} channel activation (Hua et al., 2012). Maize stomata are similar to *A. thaliana* and other plant species in that exogenous Ca^{2+} and H_2O_2 promote stomatal closure (Yao et al., 2013). We showed

that *pan2* showed fully impaired stomatal closure in response to supplemental Ca^{2+} suggesting that PAN2 is indispensable for the Ca^{2+}-dependent stomatal closure pathway. Co-immunoprecipitation and Bimolecular fluorescence complementation (BiFC) experiments showed that GHR1 physically interacts with AtSLAC1, and activates SLAC1 in a heterologous system (Hua *et al.*, 2012; Sierla *et al.*, 2018). SLAC1 is a conserved anion channel controlling turgor pressure in guard cells, thereby regulating stomatal movement in response to environmental signals in monocots and dicots (Vahisalu *et al.*, 2008). Since GHR1 is a pseudokinase (as is PAN2), its proposed effect on SLAC1 is to act as a scaffold for additional regulators rather than a direct phosphorylation activity (Sierla *et al.*, 2018). In both maize and *A. thaliana*, *slac1* mutant plants have impaired stomatal closure (Qi et al., 2018; Vahisalu et al., 2008). ZmSLAC1 is expressed explicitly in guard cells in maize (Qi *et al.*, 2018). Our expression analyses clearly indicated that PAN2 is expressed in subsidiary cells, but PAN2 expression in guard cells was less conclusive. Since guard cells and subsidiary cells have opposing turgor, and *ghr1* and *pan2* both have defects in stomatal closure, it would make sense if PAN2 action was primarily in the guard cell (rather than the subsidiary cell) - assuming the molecular function of GHR1 and PAN2 is conserved. However, this may or may not be true. PAN2 may function in subsidiary cells - perhaps regulating a SLAC1 paralog. Alternatively, PAN2 may regulate other proteins. Recently, PAN2 interactors were identified via co-immunoprecipitation/mass spectrometry in the stomatal division zone (Nan *et al.*, 2023). Amongst the high-confidence interactors were several maize proteins similar to *A. thaliana* AHA family proton transporters and a protein kinase in the SnRK family, both of which are important for stomatal function in *A. thaliana* (Nan *et al.*, 2023). Perhaps PAN2 (and GHR1?) have more general roles regulating other transporters and proteins. Both PAN2 and GHR1 are expressed in other tissues, including meristems (Zhang et al., 2012; Hua et al, 2012). An unbiased approach to identifying interactors in both stomates and other tissues will help identify the precise roles of these pseudokinases. Combining such data with future genetic and molecular work will help untangle the similar and dissimilar roles of PAN2 and GHR1. Recent single-cell gene expression analyses of maize stomatal complexes identified subsidiary cell specific genes expressed at different times in development (Sun *et al.*, 2022).

Future experiments where PAN2 is driven by promotors early in development (during subsidiary cell formation) vs later (in mature stomata) will help untangle the dual roles of PAN2. Coupled with double mutant analyses of guard cell specific and subsidiary cell specific *slac/slah* mutants will help us understand what the similar and dissimilar roles of PAN2 and GHR1 in different species and cell types.

Acknowledgments

We thank Chris Phillips, Bob Skalbite, Neal Woodward, and other greenhouse and farm staff at the University of Massachusetts Amherst for help in maintaining maize plants . We thank Ahmet Bakirbas and Stavroula Fili from Elsbeth Walker lab for their advice on the qPCR experiments. We thank Laurie Smith for reviewing our work and offering valuable feedback. This material is based upon work supported by the National Institute of Food and Agriculture, U.S. Department of Agriculture, the Center for Agriculture, Food and the Environment and the Biology Department at University of Massachusetts Amherst, under project number MAS00570. The contents are solely the responsibility of the authors and do not necessarily represent the official views of the USDA or NIFA.

Author contributions

L.L. and M.R.F. conceived the project and designed experiments. L.L., M.A.A., and T.M. performed experiments and analyzed data. L.L. and M.R.F. wrote the manuscript with the input of other authors. M.R.F. supervised the project. All the authors read and approved the final manuscript.

Conflict of interest

The authors declare that the research was conducted in the absence of any commercial or financial relationships that could be construed as a potential conflict of interest.

References cited

Allsman L, Dieffenbacher R, Rasmussen C. **2019**. Glue Impressions of Maize Leaves and Their Use in Classifying Mutants. *BIO-PROTOCOL* **9**.

Büchsenschütz K, Marten I, Becker D, Philippar K, Ache P, Hedrich R. **2005**. Differential expression of K+ channels between guard cells and subsidiary cells within the maize stomatal complex. *Planta* **222**: 968–976.

Cartwright HN, Humphries JA, Smith LG. **2009**. A Receptor-Like Protein That Promotes Polarization of an Asymmetric Cell Division in Maize. *Science* **323**: 649–651.

Dayanandan P, Kaufman PB. **1975**. STOMATAL MOVEMENTS ASSOCIATED WITH POTASSIUM FLUXES. *American Journal of Botany* **62**: 221–231.

Eyland D, van Wesemael J, Lawson T, Carpentier S. **2021**. The impact of slow stomatal kinetics on photosynthesis and water use efficiency under fluctuating light. *Plant Physiology* **186**: 998–1012.

Facette MR, Park Y, Sutimantanapi D, Luo A, Cartwright HN, Yang B, Bennett EJ, Sylvester AW, Smith LG. **2015**. The SCAR/WAVE complex polarizes PAN receptors and promotes division asymmetry in maize. *Nature Plants* **1**: 14024.

Franks PJ, Farquhar GD. **2007**. The Mechanical Diversity of Stomata and Its Significance in Gas-Exchange Control. *Plant Physiology* **143**: 78–87.

Gallagher K, Smith LG. **1999**. *discordia* mutations specifically misorient asymmetric cell divisions during development of the maize leaf epidermis. *Development* **126**: 4623–4633.

Geiger D, Scherzer S, Mumm P, Stange A, Marten I, Bauer H, Ache P, Matschi S, Liese A, Al-Rasheid KAS, *et al.*2009. Activity of guard cell anion channel SLAC1 is controlled by drought-stress signaling kinase-phosphatase pair. *Proceedings of the National Academy of Sciences* **106**: 21425–21430.

Grantz DA, Assmann SM. **1991**. Stomatal response to blue light: water use efficiency in sugarcane and soybean*. *Plant, Cell and Environment* **14**: 683–690.

Gray A, Liu L, Facette M. **2020**. Flanking Support: How Subsidiary Cells Contribute to Stomatal Form and Function. *Frontiers in Plant Science* **11**: 881.

Hanson DT, Stutz SS, Boyer JS. **2016**. Why small fluxes matter: the case and approaches for improving measurements of photosynthesis and (photo)respiration. *Journal of Experimental Botany* **67**: 3027–3039.

Hetherington AM, Woodward FI. **2003**. The role of stomata in sensing and driving environmental change. *Nature* **424**: 901–908.

Hsu P-K, Takahashi Y, Merilo E, Costa A, Zhang L, Kernig K, Lee KH, Schroeder JI. **2021**. Raf-like kinases and receptor-like (pseudo)kinase GHR1 are required for stomatal vapor pressure difference response. *Proceedings of the National Academy of Sciences* **118**: e2107280118.

Hua D, Wang C, He J, Liao H, Duan Y, Zhu Z, Guo Y, Chen Z, Gong Z. **2012**. A Plasma Membrane Receptor Kinase, GHR1, Mediates Abscisic Acid- and Hydrogen Peroxide-Regulated Stomatal Movement in *Arabidopsis*. *The Plant Cell* **24**: 2546–2561.

Humphries JA, Vejlupkova Z, Luo A, Meeley RB, Sylvester AW, Fowler JE, Smith LG. **2011**. ROP GTPases Act with the Receptor-Like Protein PAN1 to Polarize Asymmetric Cell Division in Maize. *The Plant Cell* **23**: 2273–2284.

Lawson T, Blatt MR. **2014**. Stomatal Size, Speed, and Responsiveness Impact on Photosynthesis and Water Use Efficiency. *Plant Physiology* **164**: 1556–1570.

Lawson T, Matthews J. **2020**. Guard Cell Metabolism and Stomatal Function. *Annual Review of Plant Biology* **71**: 273–302.

Long SP, Taylor SH, Burgess SJ, Carmo-Silva E, Lawson T, De Souza AP, Leonelli L, Wang Y. **2022**. Into the Shadows and Back into Sunlight: Photosynthesis in Fluctuating Light. *Annual Review of Plant Biology* **73**: 617–648.

Majore I, Wilhelm B, Marten I. **2002**. Identification of K+ Channels in the Plasma Membrane of Maize Subsidiary Cells. *Plant and Cell Physiology* **43**: 844–852.

Man J, Gallagher JP, Bartlett M. **2020**. Structural evolution drives diversification of the

large LRR-RLK gene family. *New Phytologist* **226**: 1492–1505.

Munemasa S, Hauser F, Park J, Waadt R, Brandt B, Schroeder JI. **2015**. Mechanisms of abscisic acid-mediated control of stomatal aperture. *Current Opinion in Plant Biology* **28**: 154–162.

Nan Q, Char SN, Yang B, Bennett EJ, Yang B, Facette MR. **2023**. Polarly localized WPR proteins interact with PAN receptors and the actin cytoskeleton during maize stomatal development. *The Plant Cell* **35**: 469–487.

Nunes TDG, Zhang D, Raissig MT. **2020**. Form, development and function of grass stomata. *The Plant Journal* **101**: 780–799.

Pearcy RW. Sunflecks and Photosynthesis in Plant Canopies.

Pillitteri LJ, Sloan DB, Bogenschutz NL, Torii KU. **2007**. Termination of asymmetric cell division and differentiation of stomata. *Nature* **445**: 501–505.

Qi G-N, Yao F-Y, Ren H-M, Sun S-J, Tan Y-Q, Zhang Z-C, Qiu B-S, Wang Y-F. **2018**. The S-Type Anion Channel ZmSLAC1 Plays Essential Roles in Stomatal Closure by Mediating Nitrate Efflux in Maize. *Plant and Cell Physiology* **59**: 614–623.

Raissig MT, Matos JL, Anleu Gil MX, Kornfeld A, Bettadapur A, Abrash E, Allison HR, Badgley G, Vogel JP, Berry JA, *et al.*2017. Mobile MUTE specifies subsidiary cells to build physiologically improved grass stomata. *Science* **355**: 1215–1218.

Raschke K, Fellows MP. **1971**. Stomatal movement in Zea mays: Shuttle of potassium and chloride between guard cells and subsidiary cells. *Planta* **101**: 296–316.

Schäfer N, Maierhofer T, Herrmann J, Jørgensen ME, Lind C, von Meyer K, Lautner S, Fromm J, Felder M, Hetherington AM, *et al.*2018. A Tandem Amino Acid Residue Motif in Guard Cell SLAC1 Anion Channel of Grasses Allows for the Control of Stomatal Aperture by Nitrate. *Current Biology* **28**: 1370-1379.e5.

Schindelin J, Arganda-Carreras I, Frise E, Kaynig V, Longair M, Pietzsch T, Preibisch S, Rueden C, Saalfeld S, Schmid B, *et al.*2012. Fiji: an open-source platform for biological-image analysis. *Nature Methods* **9**: 676–682.

Sierla M, Hõrak H, Overmyer K, Waszczak C, Yarmolinsky D, Maierhofer T, Vainonen JP, Salojärvi J, Denessiouk K, Laanemets K, *et al.*2018. The Receptor-like Pseudokinase GHR1 Is Required for Stomatal Closure. *The Plant Cell* **30**: 2813–2837.

Squire GR, Mansfield TA. **1972**. A SIMPLE METHOD OF ISOLATING STOMATA ON DETACHED EPIDERMIS BY LOW pH TREATMENT: OBSERVATIONS OF THE IMPORTANCE OF THE SUBSIDIARY CELLS. *New Phytologist* **71**: 1033–1043.

Suhita D, Raghavendra AS, Kwak JM, Vavasseur A. **2004**. Cytoplasmic Alkalization Precedes Reactive Oxygen Species Production during Methyl Jasmonate- and Abscisic Acid-Induced Stomatal Closure. *Plant Physiology* **134**: 1536–1545.

Sutimantanapi D, Pater D, Smith LG. **2014**. Divergent Roles for Maize PAN1 and PAN2 Receptor-Like Proteins in Cytokinesis and Cell Morphogenesis. *Plant Physiology* **164**: 1905–1917.

Vahisalu T, Kollist H, Wang Y-F, Nishimura N, Chan W-Y, Valerio G, Lamminmäki A, Brosché M, Moldau H, Desikan R, *et al.*2008. SLAC1 is required for plant guard cell S-type anion channel function in stomatal signalling. *Nature* **452**: 487–491.

Vialet-Chabrand SRM, Matthews JSA, McAusland L, Blatt MR, Griffiths H, Lawson T. **2017**. Temporal Dynamics of Stomatal Behavior: Modeling and Implications for Photosynthesis and Water Use. *Plant Physiology* **174**: 603–613.

Vico G, Manzoni S, Palmroth S, Katul G. **2011**. Effects of stomatal delays on the economics of leaf gas exchange under intermittent light regimes. *New Phytologist* **192**: 640–652.

Wang H, Guo S, Qiao X, Guo J, Li Z, Zhou Y, Bai S, Gao Z, Wang D, Wang P, *et al.*2019a. BZU2/ZmMUTE controls symmetrical division of guard mother cell and specifies neighbor cell fate in maize (S Hake, Ed.). *PLOS Genetics* **15**: e1008377.

Wang H, Yan S, Xin H, Huang W, Zhang H, Teng S, Yu Y-C, Fernie AR, Lu X, Li P, *et al.*2019b. A Subsidiary Cell-Localized Glucose Transporter Promotes Stomatal Conductance and Photosynthesis. *The Plant Cell* **31**: 1328–1343.

Willmer CM, Pallas Jr. JE. **1973**. A survey of stomatal movements and associated potassium fluxes in the plant kingdom. *Canadian Journal of Botany* **51**: 37–42.

Yao Y, Liu X, Li Z, Ma X, Rennenberg H, Wang X, Li H. **2013**. Drought-induced H2O2 accumulation in subsidiary cells is involved in regulatory signaling of stomatal closure in maize leaves. *Planta* **238**: 217–227.

Zhang X, Facette M, Humphries JA, Shen Z, Park Y, Sutimantanapi D, Sylvester AW, Briggs SP, Smith LG. **2012**. Identification of PAN2 by Quantitative Proteomics as a Leucine-Rich Repeat–Receptor-Like Kinase Acting Upstream of PAN1 to Polarize Cell Division in Maize. *The Plant Cell* **24**: 4577–4589.

Zhang L, Li D, Yao Y, Zhang S. **2020**. H2O2, Ca2+, and K+ in subsidiary cells of maize leaves are involved in regulatory signaling of stomatal movement. *Plant Physiology and Biochemistry* **152**: 243–251.

List of Supplemental Figures and Tables

Figure S1: **Comparison of stomatal developmental defects between *pan2-2* (strong allele) and *pan2-o* (weak allele).**

Figure S2. The stomatal aperture of different genotypes of leaf 8 in response to ABA.

Figure S3 PAN2 expressed in subsidiary cells and pavement cells.

Figure S4. Representative images of "curved" guard cells from pan2-2 and pan1;pan2 mutants with or without treatment with ABA

Figure S5: Relative expression levels of *PAN1* and *PAN2* in division zones and fully expanded Leaf #3, 5, and 8

Supplemental Table 1. Primer sequences for gene expression analysis.

Supplemental Table 2. Summary statistics of stomatal aperture for leaf 5 and leaf 8.

Supplemental Table 3. Results of pairwise comparisons of statistical tests for stomatal aperture for leaf 5 and leaf 8.

Supplemental Table S4. Raw CT values and calculated ratios for qRT-PCR experiments.

Supplemental Table S5. Pairwise t-tests of qRT-PCR data.

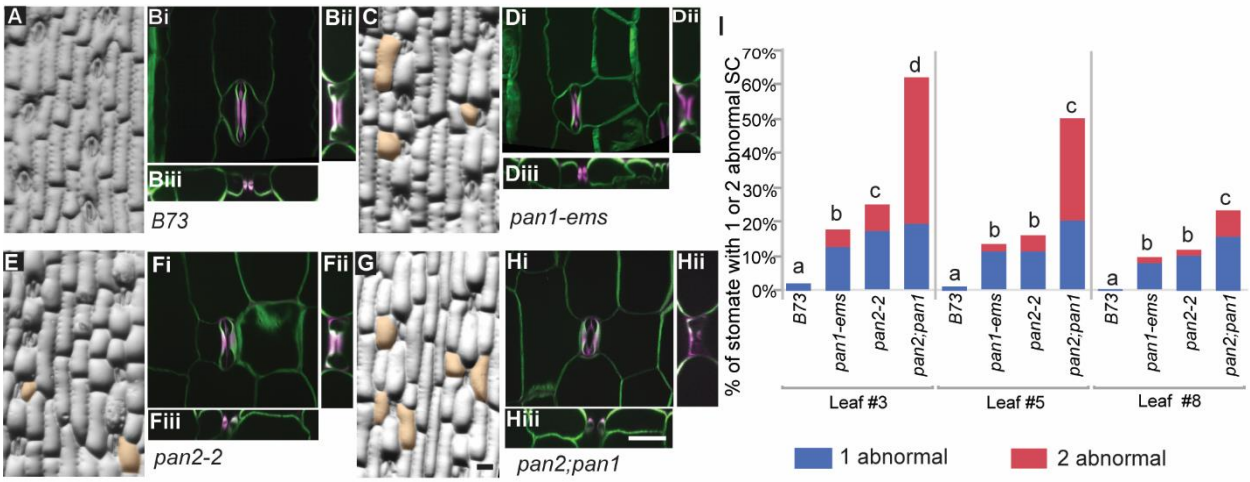

Figure 1: Mature subsidiary cells are abnormal in *pan1*, *pan2,* and *pan2;pan1* mutants.

Epidermal glue impressions (A, C, E, G) and confocal images (B, D, F, H) of wild type (A, B), *pan1* (C,D), *pan2* (E,F), and *pan2;pan1* (G,H). Abnormal subsidiaries are false-colored orange in the glue impressions. The confocal images show individual stoma stained with direct red (magenta) and calcofluor (green) and include reconstructed orthogonal views in the x (right of image) and y (below image) planes, which show the characteristic dumbbell shape of the guard cells. (E) Percentage of stomatal complexes with abnormal subsidiary cells in leaf 3, 5, and 8. Genotypes with different letters represent the percentage of stomata with one and two abnormal subsidiary cells that are significantly different from each other ($p \leq 0.05$). Statistical analysis is performed based on the student's t-test. All the representative pictures are from leaf 5. Images A, A, C, E & G are at the same scale. Images B, D, F, & H are at the same scale. Scale bars in G and H are both 50 µm.

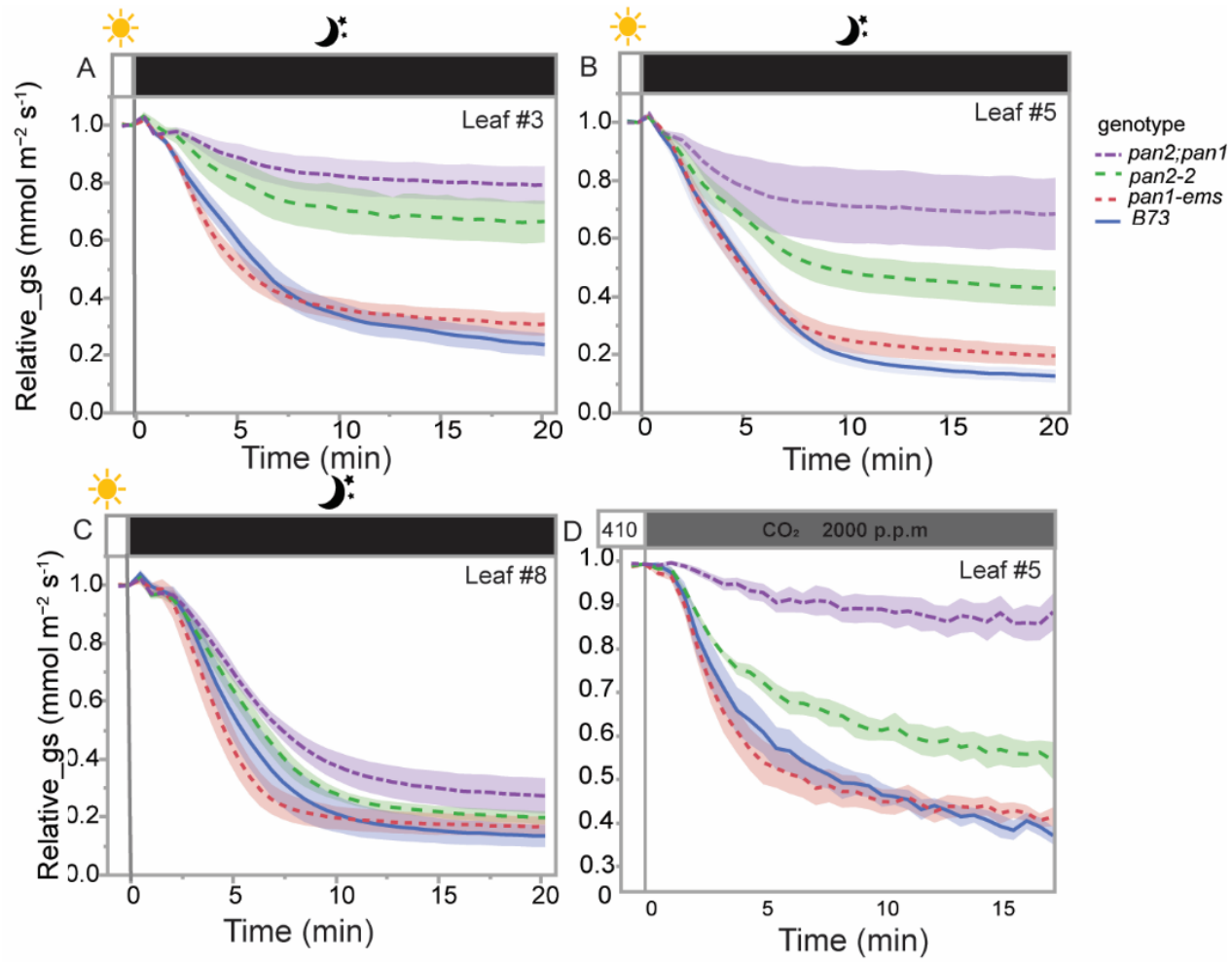

Figure 2. Stomatal closure is impaired in *pan2;pan1*, and *pan2* but is normal in *pan1*

Normalized stomatal conductance (g_s) of *pan2*, *pan2;pan*1, *pan1*, and B73 in response to darkness in leaf 3 (A), leaf 5, (B), or leaf 8 (C) was measured over time. PPFD was changed from 1000 to 0 at time zero. (D) Normalized stomatal conductance (g_s) in leaf 5 in response to elevated CO_2 was measured over time. The CO_2 concentration of from 410 ppm to 2000 ppm at zero time. Measurements were taken every 5 seconds. Relative g_s was computed for each measured plant by normalizing g_s to the observed steady initial g_s value. The data presented are the mean ± SE of at least 5 individual plants.

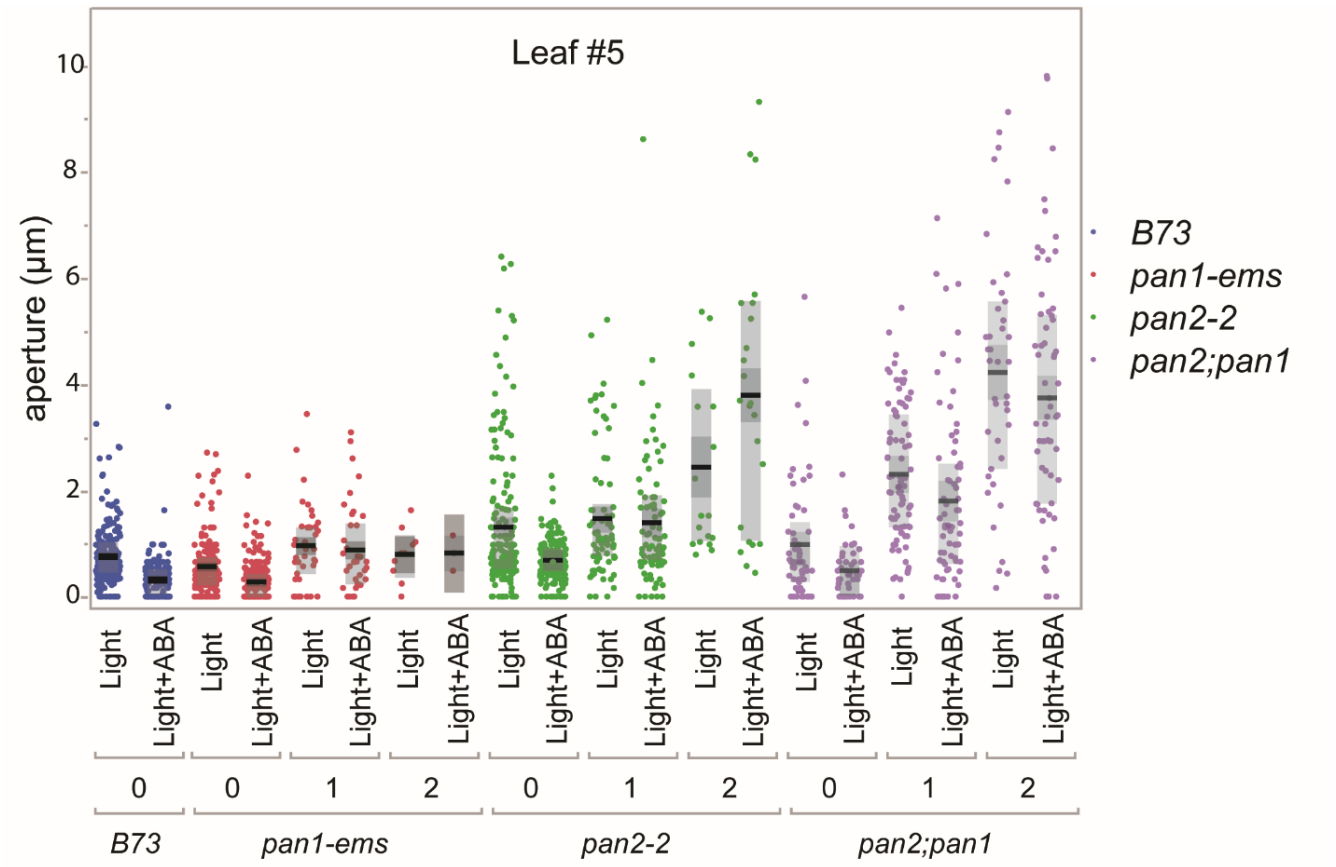

Figure 3. The stomatal aperture of different genotypes of leaf #5 in response to ABA.

Fully expanded leaf 5 segments from B73, *pan1, pan2,* or *pan2;pan1* were incubated in opening buffer under 500 µm/m^2/s light, without or with the addition of 10 mM ABA. After 2 hours, the pieces were stained with propidium iodide (PI) and imaged on the confocal microscope. Stomata were classified as having 0 abnormal (i.e., normal), 1 abnormal, or 2 abnormal subsidiary cells and stomatal apertures were measured. Each data point represents a single stomatal complex, with 3-5 plants per genotype & treatment were used.

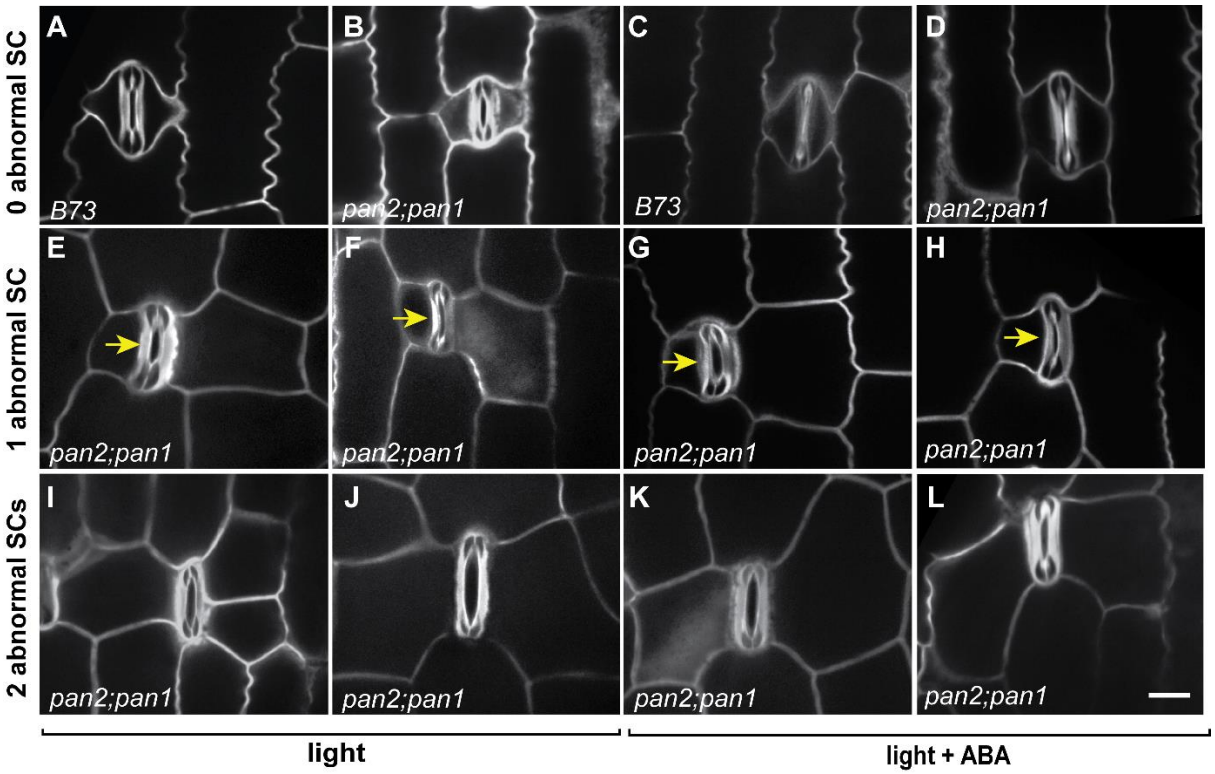

Figure 4. Curved guard cells imply that subsidiary cells exert a positive force

Leaf pieces of fully expanded leaves were treated in opening buffer in the presence or absence of 10 mM ABA. The stomata are classified into three categories based on the subsidiary morphologies. Stomata with 1 or 2 abnormalities failed to close in response to ABA treatments. The guard cells in the stoma complex with 1 abnormal subsidiary cell are curved, and all the curves are away from the normally formed subsidiary. The scale bar in L 20 µm.

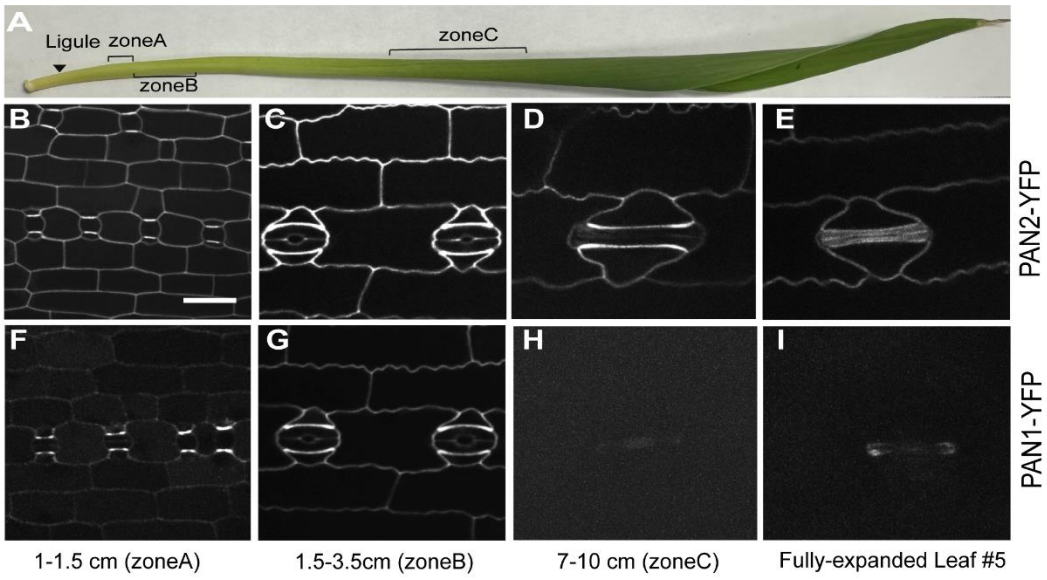

Figure 5 PAN1 and PAN2 have different expression patterns in division zones and fully expanded leaves.

The outer leaves of 15-d-old plants expressing either PAN2-YFP (B-D) or PAN1-YFP (F-H) were removed to expose partially expanded leaf 5, where the developing ligule was within 0.5 dm of the leaf base. Leaf 5 was cut into 4 sections as illustrated in A to examine expression in partially expanded leaves. The leaf blade of a fully expanded leaf 5, where the leaf sheath and leaf blade are no longer growing, were examined for PAN2-YFP (E) or PAN1-YFP (I) expression. All images at the same scale; scale bar in A represents 20 µm.

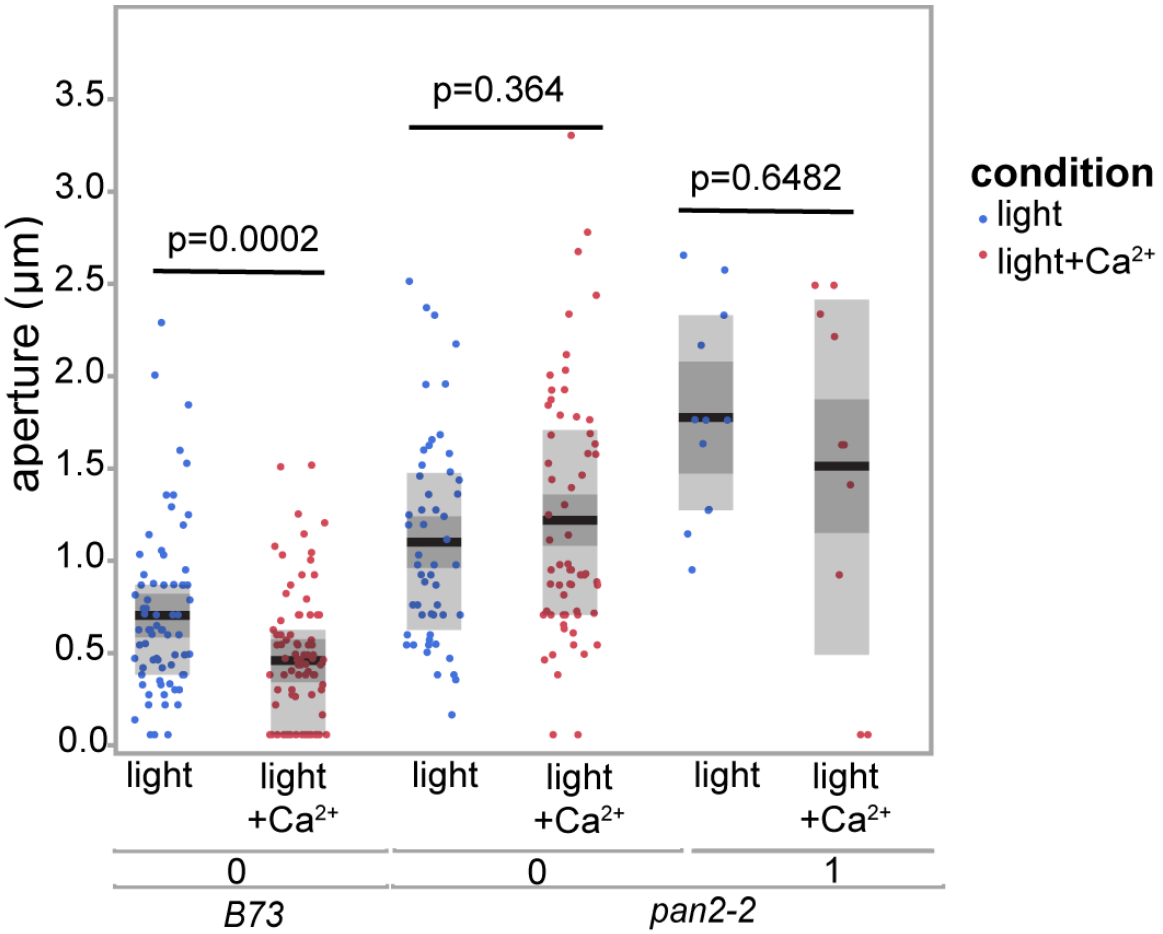

Figure 6.Stomatal aperture in *pan2* does not decrease in response to exogenous Ca^{2+}. Leaf tissue from *B73* or *pan2* was incubated in opening buffer or buffer supplemented with 100 µM Ca^{2+} under 500 µm/m^2/s light. After 2 hours, the pieces were stained with propidium iodide (PI) and imaged on the confocal microscope. Stomatal apertures were measured from the images using FIJI. Stomata were classified as having 0 abnormal (i.e., normal), 1 abnormal subsidiary cells.

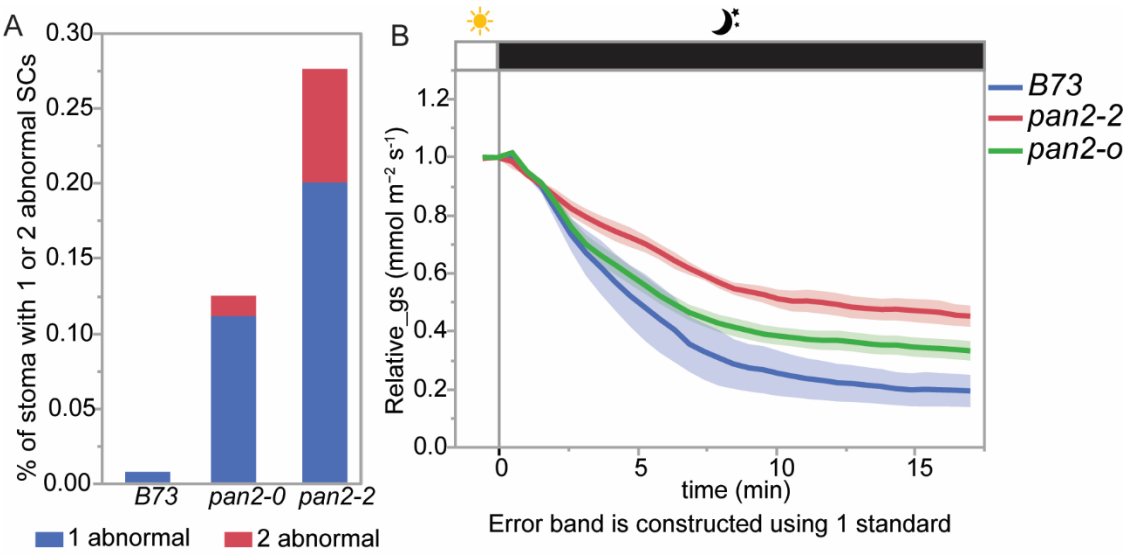

Figure S1: **Comparison of stomatal developmental defects between pan2-2 (strong allele) and pan2-o (weak allele).** (A) Percentage of abnormal cells in B73, *pan2-o,* and *pan2-2* in leaf 3*.* All the plants were planted simultaneously. At least 300 stomata complex were counted for each plant, and at least three plants were counted for each genotype. (B) The g_s of *B73*, *pan2-o*, and *pan2-2 was* measured in leaf 3 using in response to darkness. Light was turned off from 1000 to 0 at zero for the darkness response. The data presented are the mean ± SE of at least 3 individual plants. Relative g_s was computed for each measured plant by normalizing g_s to the observed steady initial g_s value. Genotypes with different letters represent the percentage of stomata with one and two abnormal subsidiary cells that are significantly different from each other ($p \leq 0.05$). Statistical analysis is performed based on the student's t-test.

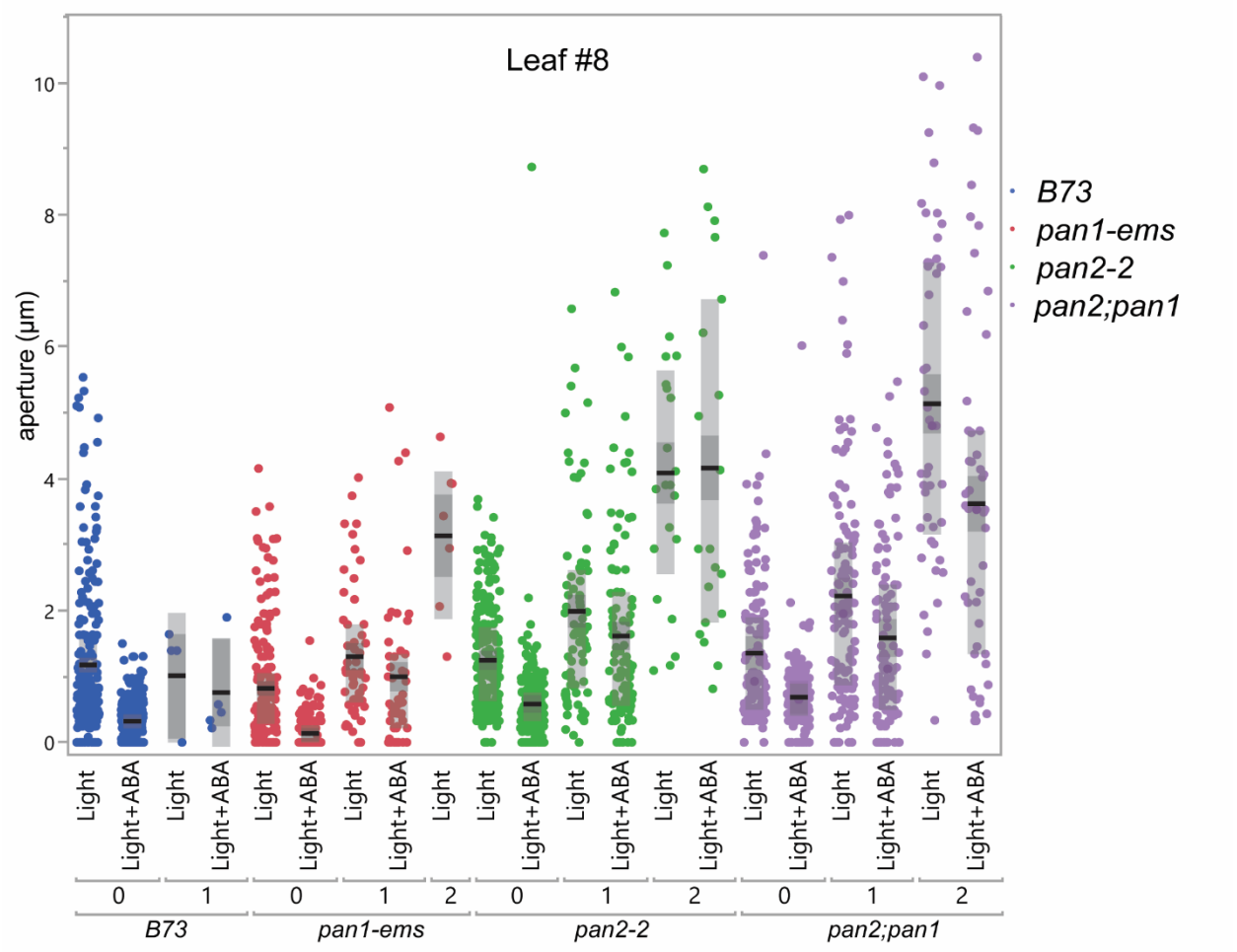

Figure S2. The stomatal aperture of different genotypes of leaf 8 in response to ABA.

Fully expanded leaf 8 segments from B73, *pan1,* or *pan1;pan2* was incubated in an opening buffer under 500 µm/m^2/s light, without or with the addition of 10 mM ABA After 2 hours, the pieces were stained with propidium iodide (PI) and imaged on the confocal microscope. Stomatal apertures were measured from the images using FIJI. Stomata were classified as having 0 abnormal (i.e., normal), 1 abnormal, or 2 abnormal subsidiary cells.

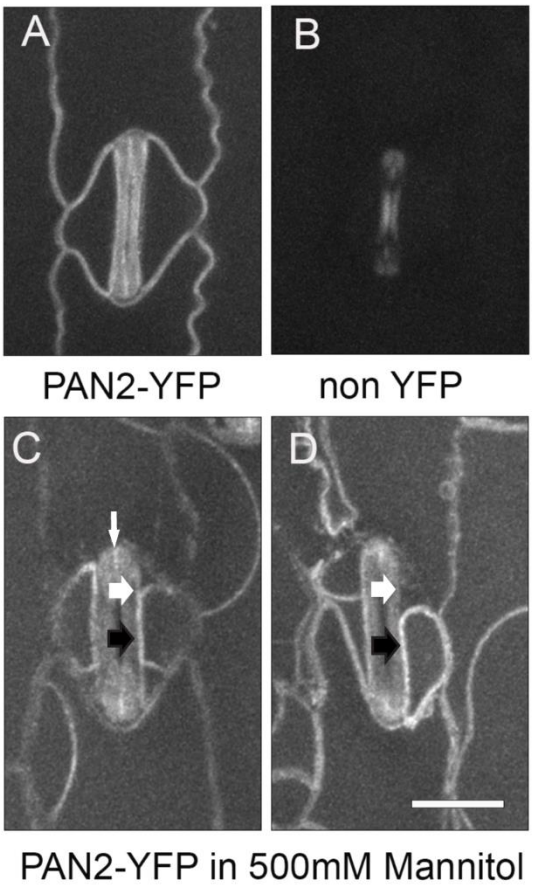

Figure S3 PAN2 expressed in subsidiary cells and pavement cells.
(A, B) Fully expanded leaf 5 was examined in transgenic maize plants expressing PAN2-YFP (A) and a sibling plant without PAN2-YFP (B). Plants were imaged on the same day with the identical acquisition settings and images were scaled identically. (C, D). Representative images of fully expanded leaf 4 tissue from plants expressing PAN2-YFP incubated in 500 mM mannitol for plasmolysis. Expression can be seen in the subsidiary cells. Black arrows indicate where the subsidiary cell plasma membrane is still adjacent to the guard cell. White arrows indicate where the subsidiary cell membrane has pulled away, indicating the membrane fluorescence in the subsidiary cell.. Scale bar = 20µm, all images scaled identically.

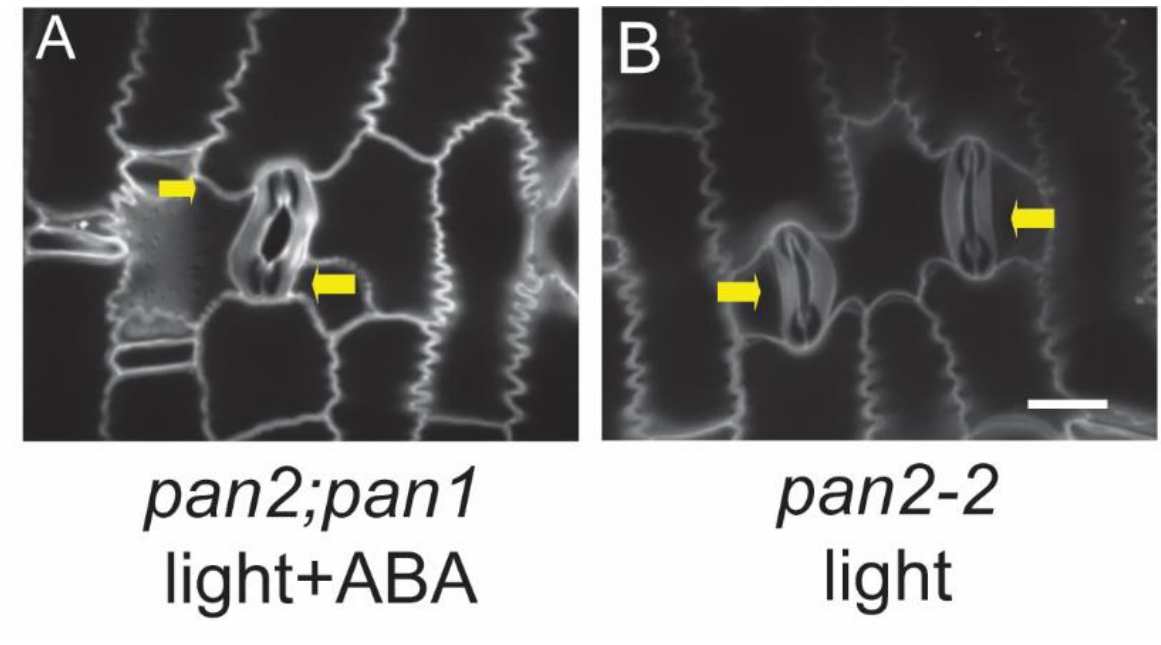

Figure S4. Representative images of "curved" guard cells from *pan2-2* and *pan1;pan2* mutants with or without treatment with ABA.

Leaf pieces of fully expanded leaves were treated in the opening buffer in the presence or absence of 10 mM ABA as figure 3 shown. The yellow arrows indicate the subsidiary cell "push" the guard cell direction. In panel A, the *pan1;pan2* guard cells are "wavy". In panel B, two stomatal complexes share a common epidermal cell that is not a subsidiary cell. The two normal subsidiary cells in the two separate complexes, which are in opposing directions, each push the associated guard cells towards the common abnormal cell. The scale bar is 20 μm.

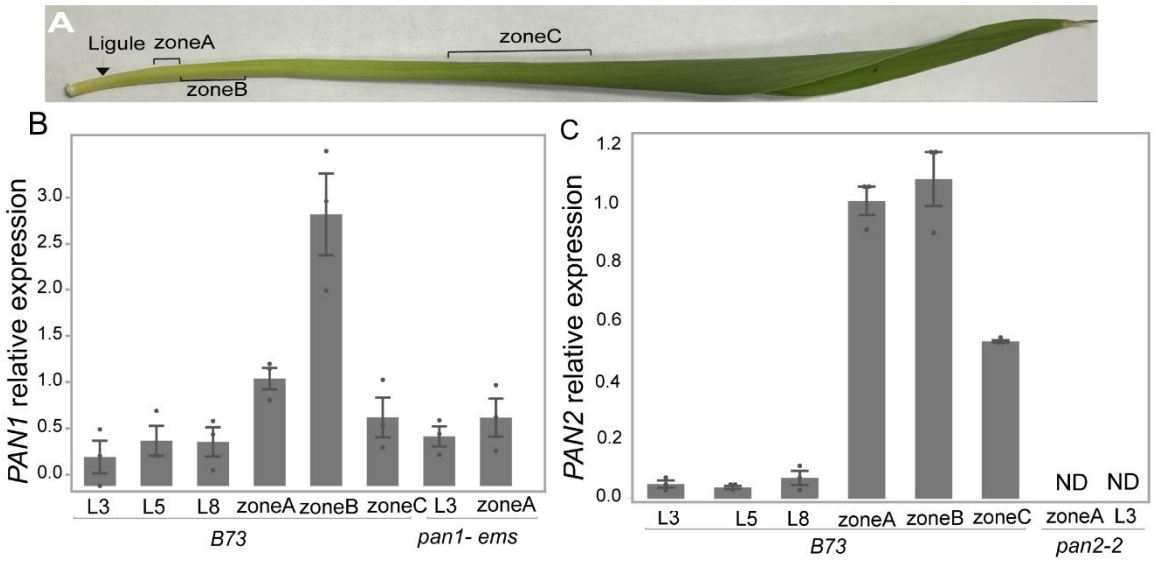

Figure S5: Relative expression levels of *PAN1* and *PAN2* in division zones and fully expanded Leaf #3, 5, and 8. (A) Diagram of developing leaf 5 showing the zones used for qRT-PCR analysis. (B) qRT-PCR analysis showing expression of PAN1 in fully expanded leaf 3 (L3), leaf 5 (L5), or leaf 8 (L8), or in leaf zones of unexpanded leaves as marked in panel A. Gene expression was measured in B73, and the *pan1-ems* null mutant was used as negative control (L3 and zone A only). (B) qRT-PCR analysis showing expression of PAN2. Labels are as in panel 1. The null mutant *pan2-2* was used as a negative control. The data are presented as mean ± SE of three biological replicates; each point represents each replicate's relative expression value. The fold change of each gene expression is computed relative to ubiquitin, and normalized relative to zone A. In *pan2-2*, one more samples had no determined ("ND") expression. Exact CT values calculated relative values, and pairwise t-tests and p-values are listed Supplementary table S3.